



Application of proton beams to radiation-induced graft polymerization for making amidoxime-type adsorbents

Kitamura, Akira ; Hamamoto, Shimpei ; Taniike, Akira ; Ohtani, Yusuke ; Kubota, Naoyoshi ; Furuyama, Yuichi

(Citation)

Radiation Physics and Chemistry, 69(2):171-178

(Issue Date)

2004-02

(Resource Type)

journal article

(Version)

Accepted Manuscript

(URL)

<https://hdl.handle.net/20.500.14094/90000434>



Application of Proton Beams to Radiation-Induced Graft Polymerization for Making Amidoxime-Type Adsorbents

Akira Kitamura*, Shimpei Hamamoto, Akira Taniike, Yusuke Ohtani,
Naoyoshi Kubota and Yuichi Furuyama

Department of Nuclear Engineering,
Kobe University of Mercantile Marine,
5-1-1 Fukaeminami-machi, Higashinada-ku, Kobe 658-0022, Japan

Abstract

MeV proton beams have been successfully applied as ionizing radiation to induce graft polymerization of acrylonitrile to prepare amidoxime-type adsorbents on polyethylene film substrates. Dependence of degree of grafting (DG) on the pre-irradiation proton energy, beam current and fluence has been examined with use of FTIR absorption measurements and RBS. The DG is observed to be proportional to the deposited energy, and saturate at a fluence of the order of 10^{13} cm^{-2} which is more than one order of magnitude smaller than the saturation fluence for molecular hydrogen release from the substrate. It is shown that graft polymerization could be possible deep into a substrate with thickness of hundreds of μm , indicating a possibility to control distribution of functional groups with a spatial variation of the order of a micron.

Key words: Proton beam, Graft polymerization, Polyethylene, Amidoxime group, FTIR, RBS

*Corresponding author: Tel.; +81-78-431-6302, Fax.; +81-78-431-6369, E-mail;
kitamura@cc.kshosen.ac.jp

1. Introduction

Graft polymerization is conveniently and effectively applied for introduction of active groups having a variety of functions onto plastic substrates of various forms; simple or porous films, nonwoven fabrics and porous microfibers. The polymerization is followed by introduction of adsorbing groups by chemically replacing the atoms on the grafted chains extending from the trunk polymer. Typical examples of the groups are; chelate-forming groups such as amidoxime groups and iminodiacetate groups suitable for collecting doubly charged ions of rare metal elements, such as uranium and vanadium, abundantly dissolved in seawater (Okamoto et al., 1985; Saito et al., 1987, 1990; Takeda et al., 1991; Sekiguchi et al., 1994; Katakai et al., 1998), affinity ligands suitable for adsorbing proteins, and sulfonic groups acting as cation-exchange groups.

Low LET (linear energy transfer) radiations such as gamma rays and electron beams are usually used to produce carbon radicals in the polymer, from which the graft polymerization is initiated. The low LET radiations have features that the irradiation is possible at the atmospheric pressure and that relatively uniform formation of the radical is expected for the specimen with a thickness of the order of mm.

In contrast, if ions having high LET and short stopping ranges are used for irradiation, a radical distribution with spatial variation of the order of nm could be expected. Due to the concentrated energy deposition, the portions having radicals could be distinctly separated from those unirradiated. This might open up a possibility of unique application of the graft polymerization technique.

When a polymer film is irradiated with ion beams, a lot of hydrogen molecules are liberated leaving chemically active tracks in the substrate. The evolution of the hydrogen release from polymers has been examined in terms of track formation (de Jong et al., 1997; Taniike et al., 2002). A variety of carbon radicals, C=C bonds, C≡C bonds and cross linking formed in the track determine the balance between retrapping reaction and recombination reaction of hydrogen radicals and thus the release of the hydrogen molecules.

In the present work ion-beam-induced graft polymerization is investigated to find features characteristic of ion beam irradiation. For this purpose dependence of DG on the ion beam parameters is studied.

2. Experimental procedure

Fig. 1 shows experimental procedure to form amidoxime-type adsorbents. Pre-irradiation of polyethylene films was made in vacuum with proton beams from a tandem pelletron accelerator 5SDH-2. The energy and current density was ranging from 2.0 to 3.12 MeV and from 0.3 to 140 nA/cm², corresponding to a fluence rate of 10⁹–10¹² cm⁻²s⁻¹, respectively, up to a fluence of 1.0×10¹²–1.0×10¹⁴ cm⁻². The films were put around a cylindrical sample holder as shown in Fig. 2, which is made of an acrylic pipe with a 15-μm-thick aluminum sheet put on the surface to extract the beam current. In some measurements the sample holder is rotated with a frequency of 12 rpm to moderate a possible inhomogeneity of the beam current density. The beam current was measured by directly monitoring the current from the aluminum foil to which a positive bias of 240

V was applied to prevent overestimation of the beam current due to secondary electron emission.

After pre-irradiation the samples were transferred in an Ar or He gas atmosphere from the vacuum chamber to a beaker filled with acrylonitrile monomer ($\text{CH}_2=\text{CHCN}$) to develop graft polymerization. The acrylonitrile was deaerated beforehand by bubbling nitrogen to passivate an anti-polymerization agent added in the commercial acrylonitrile. The gases used are not of ultra high purity.

The following procedure of chemical processing to form amidoxime groups are essentially the same as those usually employed (Saito et al., 1987, 1990). After the graft polymerization process the samples were soaked in a dimethylformamido ($\text{HCON}(\text{CH}_3)_2$) and methanol to remove residual acrylonitrile and poly(acrylonitrile) homopolymers parasitically produced.

In the amidoximation process to transform the cyano groups ($-\text{C}\equiv\text{N}$) in the grafted chains to amidoxime groups ($\text{H}_2\text{N}-\text{C}=\text{NOH}$) as chelate-forming groups, the samples were soaked in a 3 wt/v% solution of hydroxylamine hydrochloride admixture at 353 K. The solvent was an equivolume mixture of H_2O and methanol added to prevent loss of the amidoxime groups due to deformation to imidedioxime groups and hydroxamic acids, and the solution was neutralized by adding potassium hydroxide. One hour was sufficient to transform about 80 % of the cyano groups to amidoxime groups in 23- μm -thick substrates, while 6 hours were necessary for 75- μm -thick substrates.

Finally, in order to examine the adsorption characteristics some of the amidoximated samples were soaked in a 0.1 mol/cc solution of copper sulfate.

Quantitative discussions are done on the basis of weight measurement, FTIR and Rutherford backscattering spectroscopy (RBS). The degree of grafting is defined as normalized increase in weight

$$G_w = W_g / W_0 - 1, \quad (1)$$

where W_0 and W_g are the sample weight before and after polymerization, respectively. Numbers of cyano groups, amidoxime groups and adsorbed atoms introduced in each chemical process are calculated also from the weight change.

The key absorption lines in the FTIR measurements are those due to $\text{C}\equiv\text{N}$ oscillation at a wave number of 2250 cm^{-1} in the cyano groups, $\text{N}-\text{H}$ oscillation at $3100\text{--}3400 \text{ cm}^{-1}$, $\text{C}=\text{N}$ oscillation at 1640 cm^{-1} and $\text{N}-\text{O}$ oscillation at 930 cm^{-1} in the amidoxime groups.

The RBS analysis was made with use of the same accelerator as that used for the pre-irradiation. The samples were irradiated with probing beams of 3.0 MeV He^{2+} at an incident angle of 75° and a detection angle of 160° .

3. Results and discussion

3.1. Dependence of DG on ion fluence

The 23- μm -thick films were irradiated with 2 MeV protons with a fluence rate of $1.0 \times 10^{10} \text{ cm}^{-2}\text{s}^{-1}$ up to a fluence of 1.0×10^{12} to 10^{14} cm^{-2} . The DG of the films after polymerization for 8 h at 313 K is plotted in Fig. 3 as a function of the fluence. Naturally the DG increases with the

fluence, and saturates at a relatively low value of the DG compared with that in the case of electron beam irradiation.

We notice the negative value of the DG, -2% , at the lowest fluence of $1.0 \times 10^{12} \text{ cm}^{-2}$. One of the reasons for this unreasonable value seems to be due to dissolution of the polyethylene into acrylonitrile. We should assume an offset value of about -2% for all values of DG described below.

The fluence of 10^{13} cm^{-2} at which the DG begins to saturate corresponds to an energy deposition of 0.3 MGy, which is approximately equal to the dose of 0.2 MGy conventionally used in the case of electron beam pre-irradiation (Saito et al., 1987, 1990). It is anticipated from the experimental results (Taniike et al., 2002) that the hydrogen density continues to decrease on further irradiation with a proton fluence beyond $1.0 \times 10^{15} \text{ cm}^{-2}$. A possible reason for this discrepancy is discussed as follows.

Density of the alkyl radical ($-\text{CH}_2-\dot{\text{C}}\text{H}-$), which is considered to be the radical available as the starting point of the graft polymerization, increases with the ion fluence, and begins to saturate at the fluence of 10^{13} cm^{-2} . The saturation is considered to be caused by quenching of the radicals through the following mechanisms; cross linking, deformation of two alkyl radicals to a double bond of two carbons ($-\text{CH}=\text{CH}-$), and recombination with a hydrogen atom released by ion impact and diffusing around. The reaction rate in the last process is proportional to the alkyl radical density, while those in the former two are proportional to the square of the alkyl radical density. Therefore the rate of the radical quenching increases rapidly with the fluence, causing the saturation of the DG.

3.2. Dependence of DG on fluence rate

The 23- μm -thick polyethylene films were irradiated with 2.0-MeV protons up to a fluence of $3.0 \times 10^{13} \text{ cm}^{-2}$ with current densities ranging from 0.3 to 140 nA/cm^2 . Fig. 4 shows the dependence of absorbance due to the $\text{C}\equiv\text{N}$ group at 2250 cm^{-1} in the FTIR spectra on the fluence rate of the ion beam. It will be shown in the following section that the absorbance is proportional to the DG. The DG then decreases with increasing fluence rate, and appears to saturate at irradiation with a higher fluence rate. It is noticed that overlapping of the ion tracks is negligible in this range of the fluence rate. Since effective radius of the ion track is of the order of 100 nm, irradiation of the whole surface is completed in 1 ms exposure at the maximum fluence rate of $1 \times 10^{12} \text{ cm}^{-2}\text{s}^{-1}$. On the other hand, the active track is quenched within 1 μs , without waiting for overlapping by subsequent track formation.

In this series of measurements exposure time varies from 4 s for the maximum fluence rate to 6000 s for the minimum. The stability of the radical in vacuum should be checked in discussing the above data. The DGs of the samples irradiated with the same condition and kept in vacuum for different duration of time were compared for this purpose. However, no observable reduction in the DG has been found for storage up to $1.5 \times 10^4 \text{ s}$, necessitating no modification of the data in Fig.4.

It is inferred that the observed dependence of the DG on the fluence rate is caused by temperature rise due to beam heating. A rough estimation of the temperature rise at the center of the beam spot is given by a solution of the cylindrical one-dimensional equation of heat transfer. We have observed that due to deformation the portion of the beam irradiation is detached from the aluminum base which acts as a heat sink. The thermal energy then diffuses radially outward and is absorbed by a heat sink located beyond some radial distance r_2 and kept at the ambient temperature T_2 . The solution of the heat transfer equation for this idealized case is as follows:

$$T(r) = \frac{E\phi}{4K}(r_1^2 - r^2) + \frac{E\phi}{2K}r_1^2 \ln \frac{r_2}{r_1} + T_2, \quad (r \leq r_1),$$

$$T(r) = \frac{E\phi}{2K}r_1^2 \ln \frac{r_2}{r} + T_2, \quad (r_1 \leq r \leq r_2), \quad (2)$$

where E , ϕ and r_1 are the proton energy, fluence rate and the beam spot radius, respectively, and K and r_2 are the coefficient of heat transfer for the polyethylene film and an effective radius of the heat sink, respectively. Under the present beam condition, the temperature rise, $T(0)-T_2$, of 1.2×10^4 K/(Wcm⁻²), or 7.9×10^{-10} K/(cm⁻²s⁻¹) is calculated, which gives a temperature rise of greater than 80 K at the fluence rate of 1×10^{11} cm⁻²s⁻¹, where the DG begins to saturate.

The temperature rise prompts radical quenching due to enhanced diffusion of radicals resulting in enhanced rate of formation of C=C bonds and cross linking. This is considered to be a cause for the decreasing DG in the low fluence rate region. We infer that further temperature rise might stimulate revival of alkyl radicals from C=C bonds and/or cross linking, which account for the saturation of the DG in the higher fluence rate region.

3.3. Dependence of DG on ion energy

Dependence of the DG on deposited energy has been investigated by irradiating a eight-fold stack of 23-μm-thick polyethylene films with a beam of 3.12 MeV protons with a fluence rate of 2.5×10^9 cm⁻²s⁻¹ up to a fluence of 1.0×10^{13} cm⁻². The incident energies of a proton having the mean energy are 3.12, 2.85, 2.55, 2.23, 1.86, 1.43, 0.87 and 0 MeV, respectively, for each film. The range of the incident protons calculated with the Monte Carlo simulation code TRIM, 153 μm with a straggling of the order of 1 μm, lies in the seventh film. In the last film a very small fraction of energy might be deposited by δ electrons.

First, the weight loss measurement is compared with IR absorbance at 2250 cm⁻¹, which is shown in Fig. 5. With an exception of the first film marked as (1), the absorbance is approximately proportional to the weight increase with a maximum deviation of 28 %. It should be noted that a most probable fitting line does not go through the origin and appears to have an offset of about -2 % of the DG. This offset seems to have the same origin as the negative DG mentioned in Section 3.1.

Next, the DG and the IR absorbance at 2250 cm⁻¹ are plotted in Fig. 6 as a function of the deposited energy in the film. Except for the first film marked as (1) in the figure, the DG and absorbance are roughly proportional to the deposited energy.

The first film (1) has exceptionally large weight increase and absorbance extraordinarily out

of the fitting line. The beam spot on the first film is directly exposed to vacuum, and therefore to secondary electrons emitted from the wall of the beam duct and apertures. The electrons are accelerated to the target film by an electric field established by the applied positive bias and a potential induced by possible charging-up under the proton incidence. Radical production due to the electrons could be one of the reason for the excess radicals or the excess absorbance at 2250 cm^{-1} .

The first film is also subjected to accumulation of a hydrocarbon layer as a result of ion-beam-induced polymerization of residual hydrocarbon gas (Moeller et al., 1981). This could be another reason for the excess weight, although it appears that the excess absorbance at 2250 cm^{-1} of a factor of about 2 is hardly explained by this effect alone.

Next we examine a reason for scattering of the data for the radical density. In view of the relatively low DG, we suspect that a large part of the radicals were quenched during the procedure of sample transfer from the vacuum chamber to the beaker; the samples were separated from each other and soaked in the acrylonitrile separately. The variance in the number of residual radicals could occur due to the accidental quenching during the sample transfer.

To check this hypothesis, another stack of six-fold films with thickness of 13 μm was prepared. The edge portions of the films were heated and melted together to seal. The stack was pre-irradiated and soaked in the acrylonitrile without separating. After some duration of soaking the irradiated portions were cut out and subjected to measurements separately. The amount of the cyano group in each segment is shown in Fig. 7 as a function of depth along the beam trajectory, *i.e.*, in the form of depth distribution. Those at two stages of polymerization, at 250 s (the broken line, (a)) and at 3600 s (the solid line, (b)) after initiation of soaking in acrylonitrile at 353 K, are compared with deposited energy distribution shown as the dotted line. Soaking the samples longer than 1 h introduced no appreciable change in the distribution.

The number of the cyano group eventually introduced in the sample stack, the line (b), has a maximum at the central portion of the stack. There is seen no apparent dependence on the deposited energy. The nearer to the surface of the stack the film is situated, the larger the difference is between the number of the cyano group and the deposited energy. We infer that something effective for radical quenching, maybe oxygen, has diffused into the stack from both surfaces of the stack, *i.e.*, the first film and the last, during the sample transfer from the vacuum chamber to the beaker or in the acrylonitrile solution. The radical quenching and therefore the data scattering seem to occur in this process, since the oxygen invasion depends on the surface condition.

A rough estimate of the oxygen diffusion time is given here by ignoring absorption by radicals. The time-dependent diffusion equation for oxygen density $n(x, t)$ in an infinite slab with thickness of $2a$, and the initial and the boundary conditions are as follows:

$$\begin{aligned} \frac{\partial n}{\partial t} &= D_0 \nabla^2 n, \\ \text{I.C.; } n(\pm a, t) &= n_0, \end{aligned} \tag{3}$$

$$\text{B.C.}; \begin{cases} n(x,0) = 0, \text{ for } |x| < a \\ n(\pm a,0) = n_0 \end{cases},$$

where n_0 is the oxygen density in the surrounding atmosphere, and D_0 is the diffusion coefficient of oxygen in the polyethylene. The solution of this problem is given by a series expansion:

$$n(x,t) = n_0 - \sum_{s=0}^{\infty} \frac{4n_0(-1)^s}{(2s+1)\pi} \cdot \cos \frac{(2s+1)\pi}{2a} x \cdot \exp \left[- \left(\frac{(2s+1)\pi}{2a} \right)^2 D_0 t \right]. \quad (4)$$

The oxygen distribution corresponds to the difference between the distribution of radical density proportional to the deposited energy and that of residual radicals measured as absorbance due to cyano groups. Assuming a dimensionless time, $D_0 t/a^2$, and comparing those distributions, we find the most probable value of $D_0 t/a^2 = 0.5-1.0$. Using the value of the half thickness $a = 39 \mu\text{m}$ and the elapsed time t of about 3000 s during the sample transfer, D_0 is estimated to be $2.5-5.1 \times 10^{-9} \text{ cm}^2/\text{s}$. The diffusion coefficient thus derived is an effective one in a sense that it effectively involves the absorption process. The value is of the same order of magnitude as the diffusion coefficient of hydrogen in aluminum or copper. The proper value of the diffusion coefficient should be deduced from a solution of the diffusion equation with absorption taken into account.

The second point to be noticed in Fig. 7 is that the line (a) shows a different distribution from the line (b). This means that it takes about 1 h for the acrylonitrile molecule to reach the center of the stack. Again Eq. (4) can be applied for making preliminary estimate of the diffusion coefficient, D_{AO} , of the acrylonitrile molecule in the irradiated polyethylene. A rough estimate gives a rather large value of $D_{AO} = (4 \pm 2) \times 10^{-9} \text{ cm}^2/\text{s}$. It should be noted that this value is deduced again with absorption neglected.

Finally the above results mean that graft polymerization could be possible deep into a substrate with thickness of the order of hundreds of μm . This in turn implies that controlled distribution of functional groups with a spatial variation of the order of a micron could be realized by means of ion beam induced graft polymerization.

3.4. Nanoscopic characterization by RBS

To examine adsorption characteristics of the amidoximated polyethylene samples, some of them were soaked in the copper sulfate solution for more than 1 week and subjected to RBS analysis. The analysis reveals local atomic composition in the near-surface region of the order of sub-micron. Comparison with the weight measurements can be a measure of uniformity of degree of grafting, amidoximation and adsorption.

Fig. 8 shows the typical depth distributions of Cu together with N, O and C, in a 23- μm -thick sample; the third film of the eight-fold stack of polyethylene which was irradiated with 3.12 MeV protons with a fluence rate of $7.5 \times 10^9 \text{ cm}^{-2}\text{s}^{-1}$ up to a fluence of $3.0 \times 10^{13} \text{ cm}^{-2}$. The processing times for graft polymerization and amidoximation were 8 and 1 h, respectively. The distributions have been deduced on an assumption that the stopping power of the sample is the same as the

substrate polyethylene. A resolution of about 30 nm is deduced from the 12–88% width at the surface edge of the Cu spectrum. The elements other than Cu have essentially uniform distributions over the depth region probed, which implies almost uniform formation of amidoxime groups in the surface region of the substrate.

Amidoximation efficiency, η_{ao} , defined as the fraction of the cyano groups transformed to the amidoxime groups is calculated from the measured densities of O, n_O , and N, n_N :

$$\eta_{ao} = \frac{n_O}{n_N - n_O}. \quad (5)$$

Averaged values of $\eta_{ao} = 0.77$ and 0.63 are deduced from the density distributions integrated over the depth region from 0 to 300 nm and from 0 to 600 nm, respectively. The values are in good agreement with that of 0.75 calculated from the weight change. This implies that the cyano groups are replaced by amidoxime groups almost uniformly deep into the sample.

Similarly adsorption efficiency, η_a , is defined as the ratio of the atomic density of Cu, n_{Cu} , to that of O, n_O :

$$\eta_a = \frac{2n_{Cu}}{n_O}. \quad (6)$$

Averaging the Cu and O distributions from the surface to 300 nm, we find a local adsorption efficiency of $\eta_a = 0.60$. This is however larger than that of 0.13 calculated from the weight increase. One of the reason why Cu atoms are adsorbed selectively near the surface region might be that hydrophilic groups such as carboxyl groups are necessary for the Cu ions to diffuse deep into the substrate.

The DG is also expressed with use of the density ratio

$$G_w = \frac{n(2m_C + 3m_H) + m[3m_C + (3m_H + m_N)(1 + \eta_{ao}) + \eta_{ao}m_O]}{n(2m_C + 4m_H)} - 1, \quad (7)$$

where m_C , m_H , m_N and m_O are the atomic mass of C, H, N and O, respectively, and n and m are the average length of the trunk polymer $(-CH_2-CH_2-)_n$ and the average length of the grafted polyacrylonitrile chain $(-CH_2-CHCN-)_m$, respectively. With use of n and m , the ratio of the atomic density of C, n_C , to that of N, n_N , is expressed as follows:

$$\frac{n_C}{n_N} = \frac{2n + 3m}{m(1 + \eta_{ao})}. \quad (8)$$

Using Eqs. (7) and (8) together with the RBS data, the DG in the surface region from 0 to 300 nm and from 0 to 600 nm are calculated to be 33 % and 38 %, respectively. On the other hand, the weight measurements give the overall DG of 7.6 %, which is smaller by a factor of about 5. If the grafted chain were only in the surface region probed by RBS, the ratio of the DG calculated from the RBS data to that from the weight measurements would have been inverse thickness ratio of 40. This means that the graft polymerization is developed deep into the sample.

3.5. Miscellaneous consideration

The radical distribution observed in the present work has been reasonably explained by the

energy deposition profile and radical quenching by oxidation in the grafting process. The degree of grafting, however, has been relatively low. The primary reason for this appears also to be the radical quenching due to oxidation. To realize higher grafting yield and the grafted polymer distribution closer to the energy deposition profile, oxidation or unreactive peroxy radical formation should be minimized, which could be possible by more careful control of oxygen concentration and temperature of the monomer solution during the grafting process. Use of a solvent which swells polyethylene in the monomer solution could also help improving the grafting yield.

Although the dose used in the present work is rather high, the characteristic feature of the present method will be available even under low fluence irradiation. Since ion beams introduce relatively heavy damage to the host material, the effect of dose on material properties including strength is an important issue to be studied in future.

4. Conclusion

Application of MeV proton beams to induce graft polymerization of acrylonitrile in polyethylene films have been investigated. FTIR analysis and RBS together with weight measurement were employed to measure the amount of the cyano groups, the amidoxime groups and Cu atoms introduced in the sample. Dependence of the DG on the pre-irradiation proton energy, beam current and fluence has been examined.

The DG saturates at a fluence of the order of 10^{13} cm^{-2} , which is more than one order of magnitude smaller than the saturation fluence of molecular hydrogen release from the sample. This suggests that transformation of alkyl radicals available for grafting to cross linking and/or C=C double bonds proceeds on further irradiation beyond the saturation fluence. In FTIR and RBS analyses the density of the residual alkyl radical is observed to be proportional to the deposited energy but with rather large accidental variance and poor reproducibility, which is accounted for by the accidental nature of the radical quenching process during the sample transfer. It has been also shown that, although the polymerization prefers the surface region, polymerization is yet possible deep into the sample with thickness of the order of 100 μm .

Provided that the quenching of radicals is avoided, ion beams could be effectively applied to graft polymerization with a density gradient of the order of μm . This could open up a possibility to prepare functional materials having unique properties.

Acknowledgements

The authors thank Mr. T. Tokuni and T. Katoh for their help in experiments.

References

- de Jong, M. P., Maas, A. J. H., van Ijzendoorn, L. J., Klein, S. S., de Voigt, M. J. A., 1997. A model for ion-irradiation induced hydrogen loss from organic materials. *J. Appl. Phys.*, 82, 1058-1064.
- Katakai, A., Seko, N., Kawakami, T., Saito, K., Sugo, T., 1998. Adsorption of uranium in sea water using amidoxime adsorbents prepared by radiation-induced cograftering. *J. At. Energy Soc. Japan*, 40, 878-880.

- Moeller, W., Pfeiffer, Th., Schluckebier, M., 1981. Carbon buildup by ion-induced polymerization under 100-400 keV H, He and Li bombardment. Nucl. Instrum. & Meth. 182/183, 297-302.
- Okamoto, J., Sugo, T., Katakai, A., Omichi, H., 1985. Amidoxime-group-containing adsorbents for metal ions synthesized by radiation-induced grafting. J. Appl. Polym. Sci., 30, 2967-2977.
- Saito, K., Hori, T., Furusaki, S., Sugo, T., Okamoto, J., 1987. Porous amidoxime-group-containing membrane for the recovery of uranium from sea water. Ind. Eng. Chem. Res., 26, 1977-1981.
- Saito, K., Yamaguchi, T., Uezu, K., Furusaki, S., Sugo, T., Okamoto, J., 1990. Optimum preparation conditions of amidoxime hollow fiber synthesized by radiation-induced grafting. J. Appl. Polym. Sci., 39, 2153-2163.
- Sekiguchi, K., Saito, K., Konishi, S., Furusaki, S., Sugo, T., Nobukawa, H., 1994. Effect of seawater temperature on uranium recovery from seawater using amidoxime adsorbents. Ind. Eng. Chem. Res., 33, 662-666.
- Takeda, T., Saito, K., Uezu, K., Furusaki, S., Sugo, T., Okamoto, J., 1991. Adsorption and elution in hollow-fiber-packed bed for recovery of uranium from sea water.. Ind. Eng. Chem. Res., 30, 185-190.
- Taniike, A., Takeuchi, M., Kubota, N., Furuyama, Y., Kitamura, A., 2002. submitted to J. Appl. Phys.

Figure captions

- Fig. 1. Process of preparing amidoxime type adsorbent and adsorption.
- Fig. 2. Schematic of ion beam irradiation system.
- Fig. 3. Dependence of degree of grafting on fluence. Polyethylene thickness, 23 μm ; proton energy, 2.0 MeV; fluence rate, $1.0 \times 10^{10} \text{ cm}^{-2} \text{ s}^{-1}$.
- Fig. 4. Dependence of absorbance on fluence rate. Polyethylene thickness, 23 μm ; proton energy, 2.0 MeV; fluence, $3.0 \times 10^{13} \text{ cm}^{-2}$.
- Fig. 5. Relation between cyano group density and degree of grafting. Eight-fold stack of polyethylene, $8 \times 23 \text{ }\mu\text{m}$; proton energy, 3.12 MeV; fluence rate, $2.5 \times 10^9 \text{ cm}^{-2} \text{ s}^{-1}$; fluence, $1.0 \times 10^{13} \text{ cm}^{-2}$. The solid line is a guide for the eye.
- Fig. 6. Dependence of cyano group density on deposited energy. The same data of degree of grafting (closed circle) and absorbance at 2250 cm^{-1} (open circle) as those used in Fig. 5 are plotted as a function of the deposited energy. The solid line is a guide for the eye.
- Fig. 7. Distribution of cyano group in six-fold stack of 13- μm -thick polyethylene samples. Proton energy, 2.0 MeV; fluence rate, $7.0 \times 10^9 \text{ cm}^{-2} \text{ s}^{-1}$; fluence; $3.0 \times 10^{13} \text{ cm}^{-2}$. (a) Broken line: amidoximation for 250 s at 353 K, (b) solid line: amidoximation for 1 h at 353 K. The dotted line shows the energy deposition profile.
- Fig. 8. Density profiles of Cu, O, N and C deduced from an RBS spectrum of the third film of the eight-fold stack of polyethylene used in the measurements shown in Fig. 5. Graft polymerization, 8 h at 313 K; amidoximation, 1 h at 353 K.

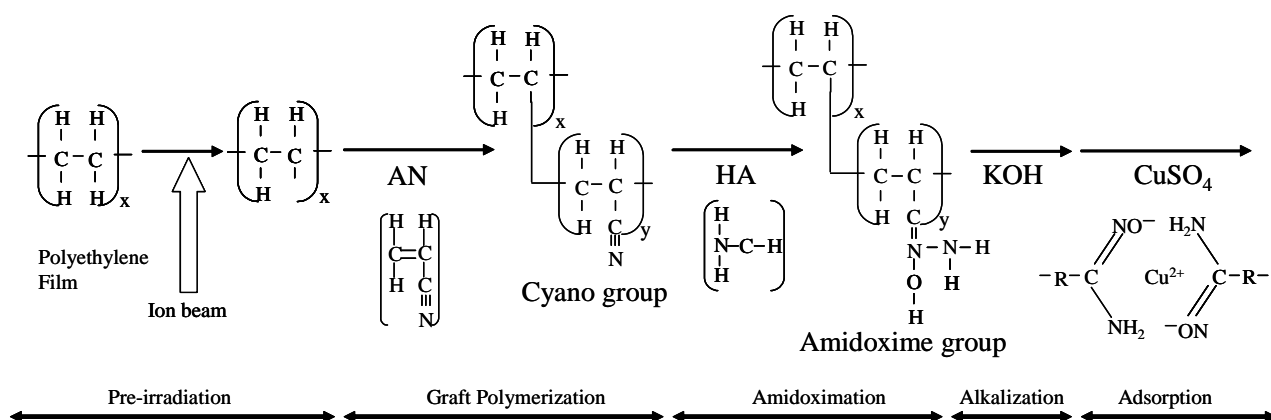


Fig. 1. Process of preparing amidoxime type adsorbent and adsorption.

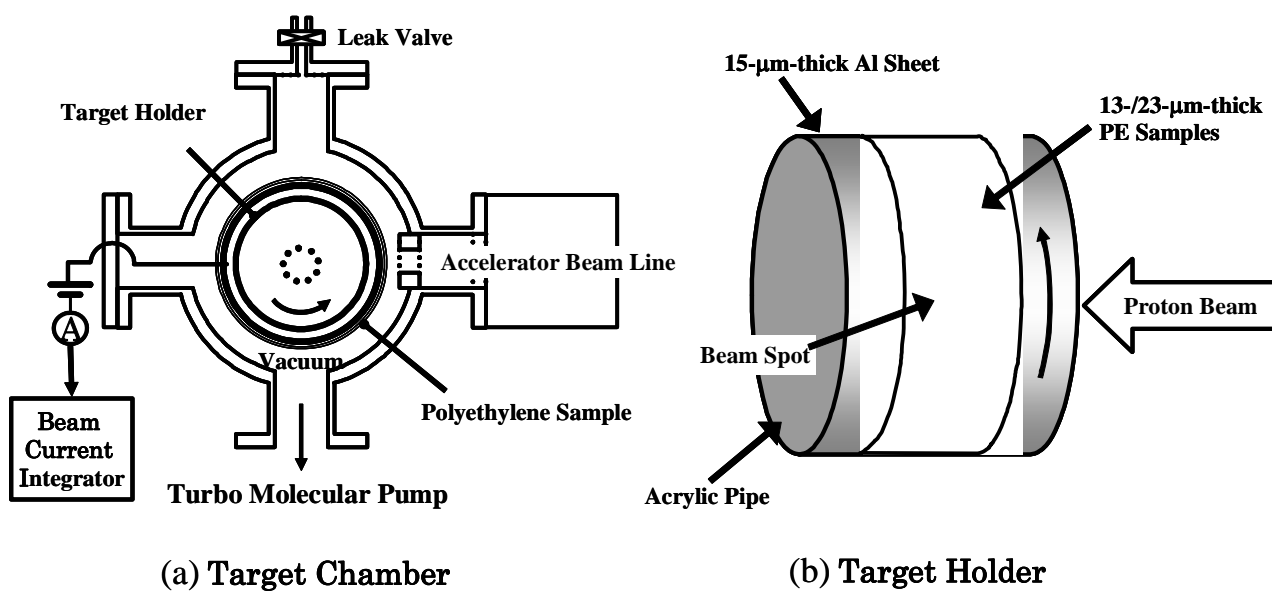


Fig.2 . Schematic of ion beam irradiation system.

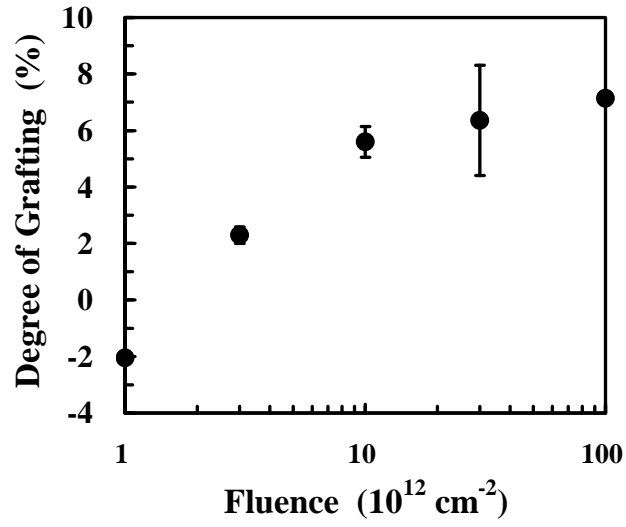


Fig. 3. Dependence of degree of grafting on fluence. Polyethylene thickness, 23 μm ; proton energy, 2.0 MeV; fluence rate, $1.0 \times 10^{10} \text{ cm}^{-2} \text{ s}^{-1}$.

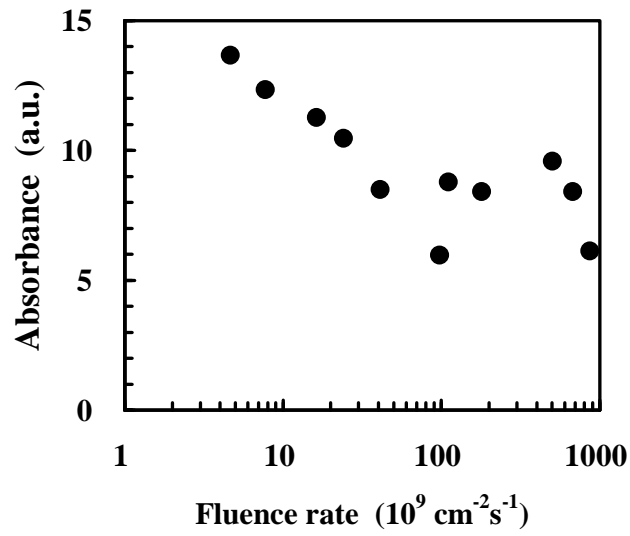


Fig. 4. Dependence of absorbance on fluence rate. Polyethylene thickness, 23 μm ; proton energy, 2.0 MeV; fluence, $3.0 \times 10^{13} \text{ cm}^{-2}$.

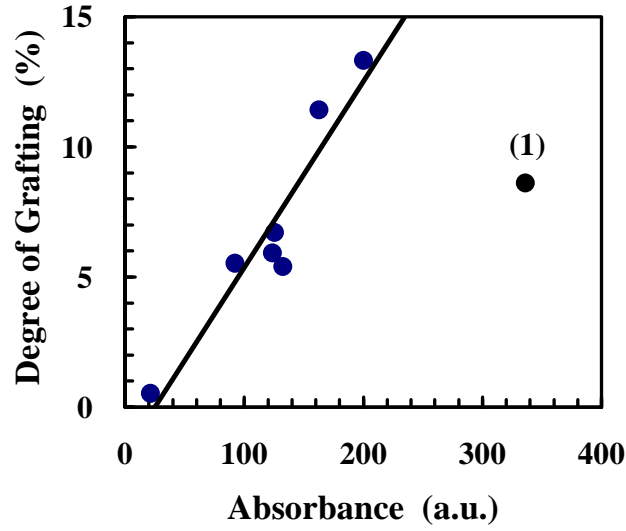


Fig. 5. Relation between cyano group density and degree of grafting. Eight-fold stack of polyethylene. $8 \times 23 \mu\text{m}$; proton energy, 3.12 MeV; fluence rate, $2.5 \times 10^9 \text{ cm}^{-2}\text{s}^{-1}$; fluence, $1.0 \times 10^{13} \text{ cm}^{-2}$. The solid line is a guide for the eye.

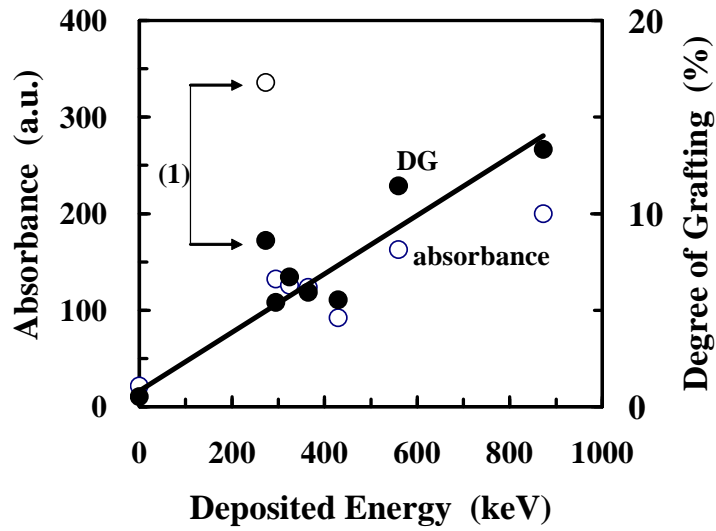


Fig. 6. Dependence of cyano group density on deposited energy. The same data of degree of grafting (closed circle) and absorbance at 2250 cm^{-1} (open circle) as those used in Fig. 5 are plotted as a function of the deposited energy. The solid line is a guide for the eye.

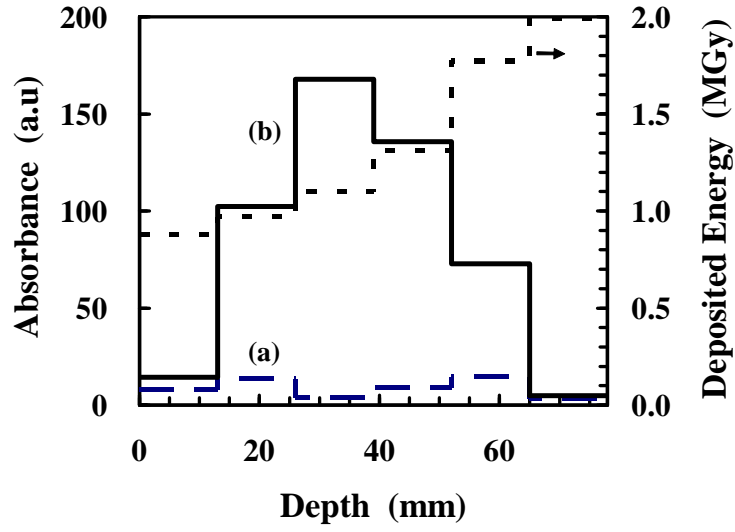


Fig. 7. Distribution of cyano group in six-fold stack of 13- μm -thick polyethylene samples. Proton energy, 2.0 MeV; fluence rate, $7.0 \times 10^9 \text{ cm}^{-2} \text{ s}^{-1}$; fluence, $3.0 \times 10^{13} \text{ cm}^{-2}$. (a) Broken line: amidoximation for 250 s at 353 K, (b) solid line: amidoximation for 1 h at 353 K. The dotted line shows the energy deposition profile.

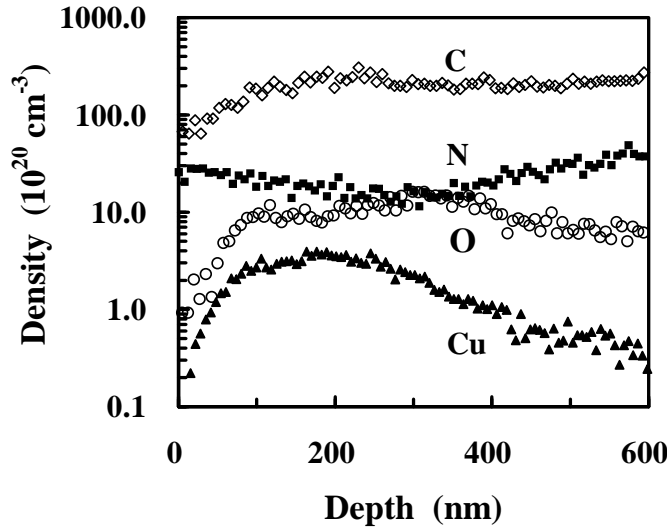


Fig. 8. Density profiles of Cu, O, N and C deduced from an RBS spectrum of the third film of the eight-fold stack of polyethylene used in the measurements shown in Fig. 5. Graft polymerization, 8 h at 313 K; amidoximation, 1 h at 353 K.